Available online at www.sciencedirect.com

SCIENCE DIRECT®

Optical Fiber Technology 12 (2006) 243–250

Optical Fiber Technology

www.elsevier.com/locate/yofte

Measurement of nonlinear and chromatic dispersion parameters of optical fibers using modulation instability

J. Fatome *, S. Pitois, G. Millot

Laboratoire de Physique de l'Université de Bourgogne (LPUB), Unité Mixte de Recherche (UMR), CNRS 5027, 9 av. A. Savary, BP 47870, 21078 Dijon, France

Received 14 March 2005; revised 15 July 2005

Available online 1 September 2005

Abstract

We present a simple method for the measurement of Kerr, second- and third-order dispersion coefficients in optical fibers using power and dispersion dependences of modulation instability near the zero-dispersion wavelength. We also complete the analysis by the accurate determination of the zero-dispersion wavelength of the fiber using the phase-matched four wave mixing process which occurs near this specific wavelength.

Keywords: Optical fiber; Nonlinearity; Modulation instability; Four wave mixing; Chromatic dispersion

1. Introduction

In ultrafast telecommunication systems using optical time division multiplexing and dispersion management techniques, picosecond and even subpicosecond pulses will be transmitted through optical fibers [1,2]. Consequently, the impact of effects such as nonlinearity, second- and third-order chromatic dispersion on transmitted pulses will be increasingly dramatic. Thus, the ability to measure the parameters responsible for these different

* Corresponding author. Fax: +33 380 395971.
E-mail address: jfatome@u-bourgogne.fr (J. Fatome).

1068-5200/$ – see front matter
doi:10.1016/j.yofte.2005.07.005

effects with a reasonable accuracy has become of great interest for the transmission-line designers and the prediction of system performance. Several methods have been proposed for measuring fiber nonlinear coefficient; most of those are based on the detection of the phase shift caused by self phase modulation (SPM), or on cross phase modulation (XPM) [3,4]. But in general, these techniques need short pulses and small chromatic dispersion; in addition, they only give access to the Kerr coefficient value. More recently, in Ref. [5], four wave mixing (FWM) was proved to be a possible way to simultaneously measure the Kerr and dispersion coefficients. This method is based on the measurements of the zero-dispersion wavelength and dispersion slope coefficient from which the chromatic dispersion is then numerically determined. Consequently, this method is dramatically dependent on zero-dispersion wavelength variations along the fiber length and very sensitive to the measurement error on dispersion slope. In Refs. [6,7], modulation instability was also proposed to measure the Kerr and dispersion coefficients but did not strictly take into account for fiber losses. We report here an extension of this method by the simultaneous measurement of Kerr, second- and third-order chromatic dispersion parameters and by using a modulation instability model taking strictly into account for fiber losses [8]. To check the accuracy of the method, we have also completed our study by a direct measurement of the zero-dispersion wavelength using FWM. We have applied our technique to the measurement of the parameters of a 12.5 km long non-zero dispersion shifted fiber (NZ-DSF). We believe that such a simple and relatively cheap technique, which allows the measurement of four different fiber parameters, could be of a great interest for future telecommunication design.

2. Experimental setup

The experimental setup is shown in Fig. 1, a continuous wave (CW) at 1550 nm was emitted by a tunable-wavelength external-cavity laser-diode (ECL). The CW was then amplified to the desired average power level by means of an erbium-doped fiber amplifier (EDFA). Stimulated Brillouin scattering (SBS) was suppressed by externally modulating the ECL with a 130-MHz sinusoidal signal applied to a $LiNbO_3$ phase modulator. This frequency was experimentally optimized to give negligible SBS back reflected power. A 95:5 coupler was placed at the amplifier output to allow for real-time monitoring of the SBS signal. The CW was finally injected in the fiber under test (standard 12.5 km long NZ-DSF)

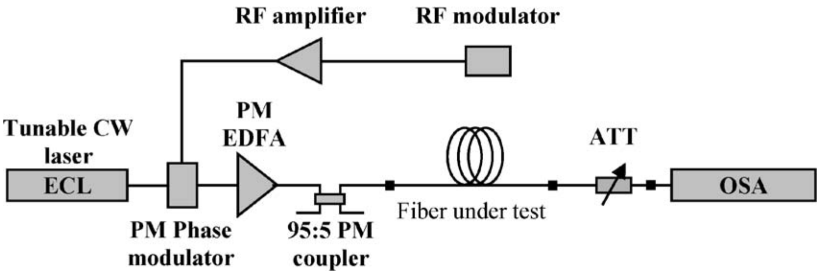

Fig. 1. Experimental setup. ATT: variable optical attenuator, PM: polarization maintained.

and the spectra of the emerging light were measured thanks to an optical spectrum analyzer (OSA) with a spectral resolution of 0.07 nm.

3. Results and discussion

The first series of measurements we carried out leads to the determination of the Kerr coefficient of a 12.5 km long NZ-DSF at 1550 nm. In absence of nonlinear losses, Raman and Brillouin effects, the dependence of the MI gain on optical power is given by [3,6]

$$G = \exp(2\gamma L_{\mathrm{eff}} P), \tag{1}$$

where γ is the Kerr coefficient of the fiber, P the input power, and L_{eff} the effective length of the fiber given by [3]

$$L_{\mathrm{eff}} = \frac{1 - \exp(-\alpha L)}{\alpha}, \tag{2}$$

where α is the fiber linear losses in m^{-1} and L the fiber length ($L_{\mathrm{eff}} = L$ in the lossless case).

From Eq. (1), the measurement of MI gain as a function of input power gives a direct access to the non-linear coefficient. The maximum MI gain was obtained by measuring the power difference between the amplified spontaneous emission (ASE) and the MI sideband peak, as can be seen in Fig. 2. Figure 3a shows the evolution of experimental MI spectrum as a function of power ranging from 120 to 270 mW, while, in Fig. 3b, we reported the corresponding measurements of G/L_{eff} as a function of power in a logarithm scale. As expected by theory, we obtained a linear curve whose slope leads to the Kerr coefficient. The best fit was obtained for $\gamma = 1.66\ \mathrm{W}^{-1}\,\mathrm{km}^{-1}$ which is close to the literature values ($1.9\ \mathrm{W}^{-1}\,\mathrm{km}^{-1}$) calculated for a DSF with the same effective area as our fiber under tested ($55\ \mu\mathrm{m}^2$) [3,6]. The accuracy of this measurement was found to be $\pm 0.04\ \mathrm{W}^{-1}\,\mathrm{km}^{-1}$ for a 99.7% confidence interval. Another series of experiments was carried out in order to determine the second- and third-order chromatic dispersion coefficients around 1550 nm owing to modulation instability. If fiber losses are taken into account, maximum MI gain in optical fiber occurs at an optimum pulsation given by [8]

$$\Omega_{\mathrm{opt}}^2 = \frac{8\omega_{\mathrm{m}}^2 P \gamma \pi c}{\lambda^2 D}, \tag{3}$$

where D is the chromatic dispersion coefficient of the fiber ($D > 0$), c the light velocity, λ its wavelength, and ω_{m}^2 is given by [8]

$$\omega_{\mathrm{m}}^2 = \frac{\exp(-\alpha L) - 1 + \alpha L}{(\alpha L)^2}. \tag{4}$$

From Eq. (4), one can easily see that $\omega_{\mathrm{m}}^2 = 1/2$ in the lossless case and $\omega_{\mathrm{m}}^2 < 1/2$ in the general case. At first, we have verified the accuracy of the model by simulating the propagation of a 400 mW continuous wave in an optical fiber with the following parameters: $D = 0.784$ ps/km nm, $\gamma = 1.7\ \mathrm{W}^{-1}\,\mathrm{km}^{-1}$, and $\alpha = 0.2$ dB/km. The MI spectrum at the fiber output is plotted in Fig. 4a. Then, in Table 1, we compare the optimum frequency

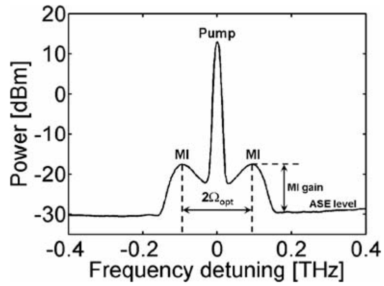

Fig. 2. Experimental MI spectrum obtained for a pump power of 200 mW at 1549.9 nm.

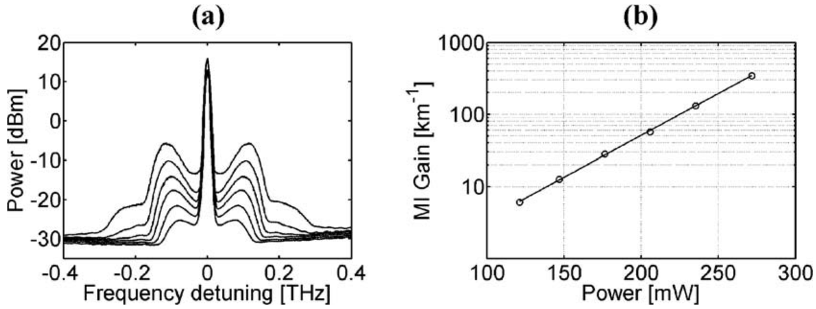

Fig. 3. (a) Evolution of the MI sidebands at 1550 nm as a function of input power, from bottom to top, $P = 120$, 145, 175, 205, 235, and 270 mW. (b) Evolution of MI gain as a function of input power, measurements (circles) and linear fit (solid line).

detuning Ω_{opt} obtained from this numerical simulation with the Karlson model [8], the lossless model [3] and the 0.86 linear losses corrective term of Ref. [7]. Thus, we can clearly see that only the Karlson model [8] gives the accurate value of the optimum MI frequency detuning while other models lead to an error larger than 5%.

The tunable properties of our laser-diodes were used to measure the optimum MI frequency as a function of wavelength from 1540 to 1560 nm for a fixed input power of 225 mW. Figure 4b shows the evolution of the MI spectrum for the three different wavelengths, 1540, 1550, and 1560 nm. Since the Kerr coefficient is known from the previous study and does not significantly depend on λ, we directly calculated for each wavelength the second-order chromatic dispersion coefficient, D, owing to Eq. (3). Figure 4c illustrates the experimental evolution of D as a function of wavelength. As can be seen, the evolution is linear and the value of D at 1550 nm, 1.00 ± 0.06 ps/km nm, is close to the manufacturer value 1.21 ps/km nm. Therefore, as the zero-dispersion wavelength of the NZ-DSF is close to the measurement wavelengths, and as the fiber dispersion seems to have a strictly linear slope, the third-order chromatic dispersion coefficient, S around 1550 nm, was directly evaluated by fitting the linear curve of the second-order chromatic dispersion parameter, D, as a function of wavelength. S was found to be 0.070 ± 0.005 ps/km nm^2 which is also in good agreement with the manufacturer value 0.069 ps/km nm^2. Finally, thanks to both the value of D at 1550 nm and S, the zero-dispersion wavelength, λ_0, was also evaluated and

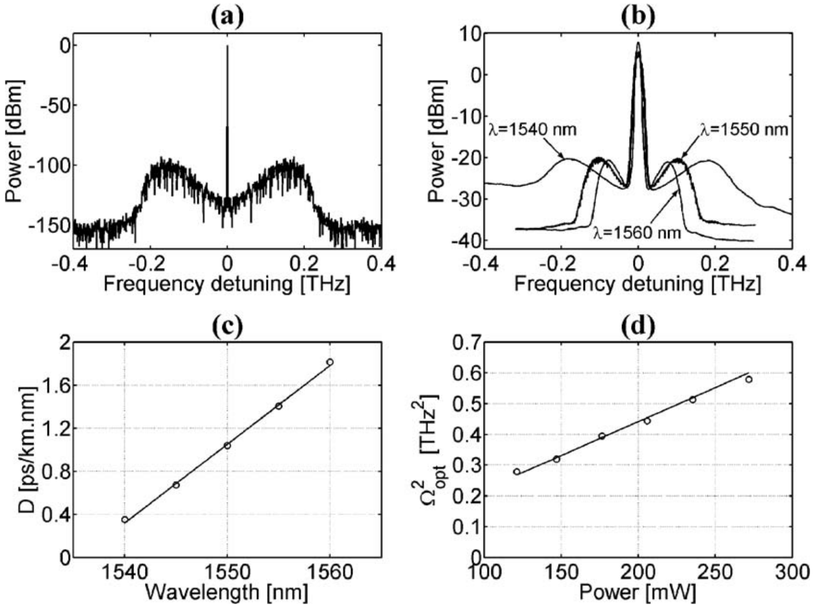

Fig. 4. (a) MI spectrum obtained from numerical simulation with $D = 0.784$ ps/km nm, $\gamma = 1.7\ \mathrm{W}^{-1}\,\mathrm{km}^{-1}$, $\alpha = 0.2$ dB/km, and $L = 12.5$ km. (b) Evolution of the MI sidebands as a function of wavelength (1540, 1550, and 1560 nm) for an input power of 225 mW. (c) Dispersion of the fiber under test as a function of wavelength, measurements (circles) and linear fit (solid line). (d) Comparison between the power dependence of the MI frequency detuning obtained from Eq. (3) (solid line) and experiments (circles) at 1550 nm.

Table 1
Frequency detuning obtained from numerical simulation, from the Karlson model [8], from the lossless model [3] and from the corrective term of Ref. [7]

Model	MI frequency detuning (GHz)
Numerical simulation	168
Karlson model [8]	169.4
Lossless model [3]	185.6
Correction of Ref. [7]	159.6

found to be 1535.7 ± 1.9 nm. Then, we plot in Fig. 4d the power dependence of the MI frequency detuning obtained from Eq. (3) owing to the previously found fiber parameters (solid line) as well as those measured experimentally (circles). The good agreement between the two different curves proves the validity of the Karlson model and the accuracy of our measurements.

In order to check the reliability of the MI method, the full characterization of the fiber was finally completed by the independent determination of the zero-dispersion wavelength, λ_0. To obtain this value, we take advantage of the degenerated four wave mixing (FWM) process occurring near this specific wavelength. Indeed, the generation of an idler wave from the nonlinear interaction between a pump wave at frequency f_p (wavelength λ_p)

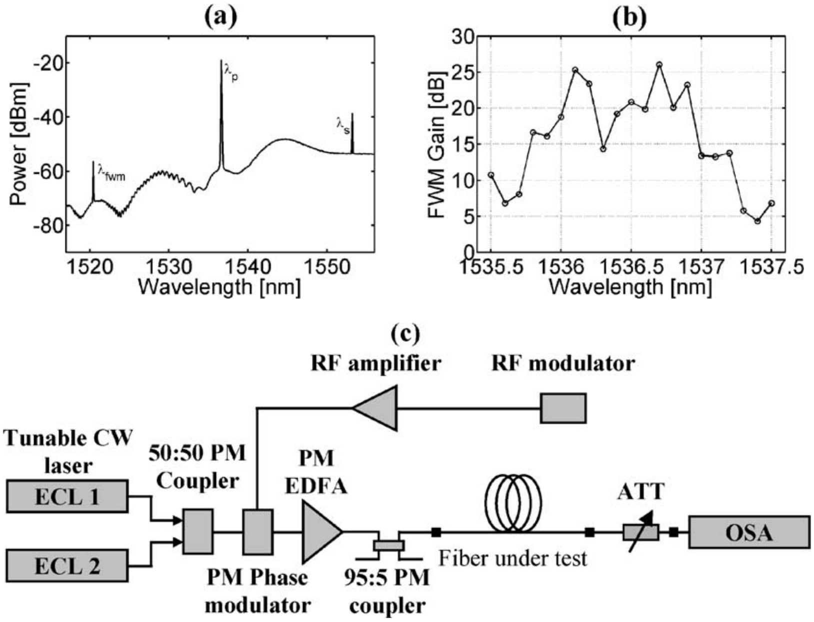

Fig. 5. (a) Spectrum of the FWM process when the pump wavelength is near the zero dispersion. $\lambda_p = 1536.7$ nm, $P_p = 80$ mW, $\lambda_s = 1532$ nm, and $P_s < 1$ mW. (b) FWM efficiency as a function of pump wavelength near the zero dispersion. (c) Experimental setup of the zero-dispersion measurement technique.

and a signal wave at frequency f_s (wavelength λ_s) near the zero-dispersion frequency f_0 (wavelength λ_0) is ruled by the following FWM phase-matched condition [3]:

$$f_p - f_0 = -\frac{\pi\beta_4(f_s - f_0)^2}{6\beta_3}, \tag{5}$$

where β_3 and β_4 are respectively the third- and fourth-order dispersion coefficients. Let us emphasize that Eq. (5) remains valid as long as pump depletion can be neglected. On the other hand, one can demonstrate [9] that the FWM efficiency, i.e., the idler signal gain, is maximum when the pump wavelength is equal to the zero-dispersion wavelength and rapidly decreases as the pump wavelength is detuned from λ_0. Moreover, the frequency bandwidth of the FWM gain curve is also dependent on the wavelength detuning between the pump and the signal [9]. Especially, the bandwidth becomes narrower for large differences [9], which is suitable for a better measurement precision. In our experiment, the pump-signal detuning was fixed to 15 nm. Figure 5a illustrates the experimental generation of an idler wave at wavelength λ_{fwm} from the FWM process described above. Figure 5c shows the experimental setup of the zero-dispersion measurement technique. It is roughly the same than the one described in Fig. 1 except that we used two continuous waves (pump and signal) combined by a fiber fused 50:50 coupler. The use of polarization maintained (PM) equipments allowed us to inject both waves into the optical fiber with parallel linear states of polarization. This polarization configuration increases the efficiency of the FWM process into the NZ-DSF. We measured the idler sideband gain as a function of the pump wavelength for a signal fixed to 1553 nm. Figure 5b shows the evolution of the FWM efficiency as a function of the pump wavelength. Because of the zero-dispersion wavelength fluctuations along the fiber length, the FWM phase-matching condition is never fully satisfied. Consequently, we did not observe a narrow single peak gain centered on λ_0, but a complex pattern as expected in Ref. [9]. The centered wavelength of this complex pattern was set to be the average zero-dispersion wavelength of the fiber and was evaluated to 1536.5 nm which is in good agreement with the previous result obtained from MI measurements, 1535.7 ± 1.9 nm thus, confirming the reliability of our method.

4. Conclusion

In this paper, we have reported a simple method for the simultaneous determination of the Kerr, second-, third-order chromatic dispersion coefficients and zero-dispersion wavelength in optical fibers using power and dispersion dependences of modulation instability. More especially, we have clearly shown the necessity to take carefully into account for fiber losses in the model for an accurate determination of those parameters. Furthermore, we have also completed the characterization of the fiber under test by the independent determination of the zero-dispersion wavelength using the satisfied phase-matching condition of four wave mixing near this specific wavelength. The good agreement between the results obtained from the modulation instability (MI) and four wave mixing (FWM) methods finally consolidates our measurements. The main limitation of our technique is that the measurement of the nonlinear coefficient does not take into account for pump depletion, so one should find a trade off between the pump power and the fiber length to avoid any mistake. Second, strong dispersion variations along the fiber length could affect the measurements by increasing the MI gain bandwidth and decreasing the maximum MI gain. In conclusion, we believe that such a simple and cheap method could be of a great help for telecommunication engineers and transmission-line designers.

References

[1] M. Nakazawa, T. Yamamoto, K. Tamura, 1.28 Tbit/s—70 km OTDM transmission using third- and fourth-order simultaneous dispersion compensation with a phase modulator, Electron. Lett. 36 (24) (2000) 2027–2029.
[2] A.H. Gnauck, G. Raybon, P.G. Bernasconi, J. Leuthold, C.R. Doerr, L.W. Stulz, 1-Tb/s (6×170.6 Gb/s) transmission over 2000-km NZDF using OTDM and RZ-DPSK format, IEEE Photon. Technol. Lett. 15 (11) (2003) 1618–1620.
[3] G.P. Agrawal, Nonlinear Fiber Optics, third ed., Academic Press, New York, 2001.
[4] K.S. Kim, R.H. Stolen, Measurement of the nonlinear index of silica-core and dispersion-shifted fibers, Opt. Lett. 19 (4) (1994) 257–259.
[5] H. Chen, Simultaneous measurements of non-linear coefficient, zero-dispersion wavelength and chromatic dispersion in dispersion-shifted fibers by four-wave mixing, Opt. Commun. 220 (2003) 331–335.
[6] M. Artiglia, E. Ciaramella, B. Sordo, Using modulation instability to determine Kerr coefficient in optical fibres, Electron. Lett. 31 (12) (1995) 1012–1013.
[7] M. Artiglia, E. Ciaramella, Characterization of modulation instability gain in optical fibres, in: Optical Fiber Measurement Conference (OFMC), vol. 5, 1995.

[8] M. Karlson, Modulational instability in lossy optical fibers, J. Opt. Soc. Amer. B 12 (11) (1995) 2071–2077.
[9] K. Inoue, Four-wave mixing in an optical fiber in the zero-dispersion wavelength region, J. Lightwave Technol. 10 (11) (1992) 1553–1561.